

<https://helda.helsinki.fi>

High spatiotemporal variability of methane concentrations challenges estimates of emissions across vegetated coastal ecosystems

Roth, Florian

2022-07

Roth , F , Sun , X , Geibel , M C , Prytherch , J , Bruchert , V , Bonaglia , S , Broman , E , Nascimento , F , Norkko , A & Humborg , C 2022 , ' High spatiotemporal variability of methane concentrations challenges estimates of emissions across vegetated coastal ecosystems ' , Global Change Biology , vol. 28 , no. 14 , pp. 4308-4322 . <https://doi.org/10.1111/gcb.16177>

<http://hdl.handle.net/10138/345339>

<https://doi.org/10.1111/gcb.16177>

cc_by

publishedVersion

Downloaded from Helda, University of Helsinki institutional repository.










This is an electronic reprint of the original article.

This reprint may differ from the original in pagination and typographic detail.

Please cite the original version.

RESEARCH ARTICLE

High spatiotemporal variability of methane concentrations challenges estimates of emissions across vegetated coastal ecosystems

Florian Roth^{1,2}  | Xiaole Sun^{1,3}  | Marc C. Geibel¹ | John Prytherch⁴  |
Volker Brüchert^{5,6}  | Stefano Bonaglia⁷  | Elias Broman^{1,8}  |
Francisco Nascimento^{1,8}  | Alf Norkko^{1,2}  | Christoph Humborg^{1,2} 

¹Baltic Sea Centre, Stockholm University, Stockholm, Sweden

²Tvärminne Zoological Station, University of Helsinki, Hanko, Finland

³Center of Deep Sea Research, Institute of Oceanology, Chinese Academy of Sciences, Qingdao, China

⁴Department of Meteorology, Stockholm University, Stockholm, Sweden

⁵Department of Geological Sciences, Stockholm University, Stockholm, Sweden

⁶Bolin Centre for Climate Research, Stockholm University, Stockholm, Sweden

⁷Department of Marine Sciences, University of Gothenburg, Gothenburg, Sweden

⁸Department of Ecology, Environment and Plant Sciences, Stockholm University, Stockholm, Sweden

Correspondence

Florian Roth, Baltic Sea Centre, Stockholm University, Stockholm, Sweden.

Email: florian.roth@su.se

Funding information

The study was funded by the Academy of Finland (Project ID 294853) and is part of the University of Helsinki and Stockholm University collaborative research initiative (The Baltic Bridge initiative) and further supported by the Walter and Andrée de Nottbeck Foundation. Financial support was provided by the Swedish Research Council Formas to EB (grant no: 2020-02304).

Abstract

Coastal methane (CH₄) emissions dominate the global ocean CH₄ budget and can offset the “blue carbon” storage capacity of vegetated coastal ecosystems. However, current estimates lack systematic, high-resolution, and long-term data from these intrinsically heterogeneous environments, making coastal budgets sensitive to statistical assumptions and uncertainties. Using continuous CH₄ concentrations, δ¹³C-CH₄ values, and CH₄ sea–air fluxes across four seasons in three globally pervasive coastal habitats, we show that the CH₄ distribution is spatially patchy over meter-scales and highly variable in time. Areas with mixed vegetation, macroalgae, and their surrounding sediments exhibited a spatiotemporal variability of surface water CH₄ concentrations ranging two orders of magnitude (i.e., 6–460 nM CH₄) with habitat-specific seasonal and diurnal patterns. We observed (1) δ¹³C-CH₄ signatures that revealed habitat-specific CH₄ production and consumption pathways, (2) daily peak concentration events that could change >100% within hours across all habitats, and (3) a high thermal sensitivity of the CH₄ distribution signified by apparent activation energies of ~1 eV that drove seasonal changes. Bootstrapping simulations show that scaling the CH₄ distribution from few samples involves large errors, and that ~50 concentration samples per day are needed to resolve the scale and drivers of the natural variability and improve the certainty of flux calculations by up to 70%. Finally, we identify northern temperate coastal habitats with mixed vegetation and macroalgae as understudied but seasonally relevant atmospheric CH₄ sources (i.e., releasing ≥ 100 μmol CH₄ m⁻² day⁻¹ in summer). Due to the large spatial and temporal heterogeneity of coastal environments, high-resolution measurements will improve the reliability of CH₄ estimates and confine the habitat-specific contribution to regional and global CH₄ budgets.

KEYWORDS

blue carbon, carbon cycle, climate change, coastal greenhouse gas emissions, methane fluxes

This is an open access article under the terms of the [Creative Commons Attribution](https://creativecommons.org/licenses/by/4.0/) License, which permits use, distribution and reproduction in any medium, provided the original work is properly cited.

© 2022 The Authors. *Global Change Biology* published by John Wiley & Sons Ltd.

1 | INTRODUCTION

Methane (CH₄) is the second most important greenhouse gas (GHG) driving global climate change (Shindell et al., 2009). Past research has shown that coastal marine environments dominate the global ocean CH₄ budget and contribute 5–28 Tg CH₄ yr⁻¹ to total global CH₄ emissions (Rosentreter et al., 2021b; Weber et al., 2019). However, a scarcity of systematic, high-resolution, and long-term measurements has hampered our ability to confine CH₄ emissions from a wide range of heterogeneous and dynamic coastal environments impeding efforts to evaluate the potential of coastal ecosystems to mitigate climate change by storing carbon (Rosentreter et al., 2021a).

Particularly in coastal sediments, CH₄ can be produced in large amounts due to the organic carbon surplus of primary production from submerged (e.g., seagrass and macroalgae) and partially emerged (e.g., mangroves and salt marshes) vegetation (Duarte et al., 2005; Ortega et al., 2019; Snelgrove et al., 2018) and the accumulation of allochthonous particulate organic matter (Barnes & Goldberg, 1976; Reeburgh, 1983; Wallenius et al., 2021). In such environments, CH₄ emissions can offset or even negate the value of coastal ecosystems as "blue carbon" storage reservoirs by counteracting carbon fixation and burial (Rosentreter et al., 2018). However, stretching over a global coastline of ~1,600,000 km, these environments are intrinsically heterogeneous with a mosaic of habitats with varying substrate composition (Holland & Elmore, 2008; Koch, 2001), associated species communities (Dias et al., 2018; Stein et al., 2014), and ecosystem processes across space and time (Cardinale et al., 2006; Hewitt et al., 2008). Thus, the inherent properties that make coastal environments so diverse and heterogeneous also complicate our ability to narrow down carbon dynamics in these areas sufficiently (Rosentreter et al., 2021a).

In this context, global estimates of coastal CH₄ emissions presently do not sufficiently reflect the heterogeneous and dynamic nature of coastal environments. In fact, the three classical blue carbon ecosystems, seagrass meadows, salt marshes, and mangrove forests (Mcleod et al., 2011) have been the focal point for global coastal CH₄ assessments due to their large carbon sequestration potential (Mcleod et al., 2011). It is only recently that tidal flats, coastal aquaculture, and inner estuaries have been added to the global CH₄ budget (Rosentreter et al., 2021b), but measurements from other coastal areas are still pooled without further habitat discrimination (Weber et al., 2019). For example, highly productive but less conspicuous coastal ecosystems with mixed-macrophytes, algal dominance, or bare sediments are common but not explicitly included in these estimates. Yet, given their high carbon turnover rates (Attard et al., 2019a, 2019b), these habitats may contribute significantly to the total coastal CH₄ emissions (Lundevall-Zara et al., 2021). Moreover, the majority (85%) of studies quantifying CH₄ emissions from vegetated coastal areas have been performed south of 45 degrees North (70% when excluding mangroves that only occur around the tropics) (Al-Haj & Fulweiler, 2020). Northern temperate and high-latitude coastal systems are highly productive and also experience climate change at an accelerated rate compared to low- and mid-latitude

areas (Screen & Simmonds, 2010; Serreze et al., 2009), increasing the demand for studies assessing temperature-sensitive CH₄ dynamics from these regions (Yvon-Durocher et al., 2014). There is also a major knowledge gap in our understanding of the variability of CH₄ in surface waters over short spatial scales reflecting the ecosystem mosaic typical for the coastal environment (Sheaves, 2009), as has been shown relevant for seafloor gross primary production and community respiration in shallow areas (Rodil et al., 2021).

Emissions of CH₄ are, furthermore, particularly variable in time, and narrowing the uncertainty in the global coastal CH₄ budget requires a methodology capable of quantifying natural variations arising from biotic and abiotic drivers across multiple timescales (Rosentreter et al., 2021a). For example, 74 of 98 studies (75.5%) used to calculate the global median CH₄ flux from vegetated coastal ecosystems in Al-Haj and Fulweiler (2020) employed flux chamber measurements or discrete sampling. Chamber measurements produce time-averaged flux estimates (often for a period between 24 and 48 h). In contrast, discrete samples have no time-weighted average, but due to logistical reasons, are usually taken at frequencies of no more than one to five samples per day and location (Banerjee et al., 2018; Dutta et al., 2015; Nirmal Rajkumar et al., 2008). These studies resulted in significant advances in our understanding of CH₄ emission from coastal systems. Yet, the strong influence of physical forcing (e.g., wind, waves, currents, tides) on the main CH₄ emission pathways (diffusion and ebullition) over short timescales (minutes to hours) can lead to a high CH₄ concentration and flux variability within one diel cycle, as has been shown in lake environments (Sieczko et al., 2020) and tidal influenced estuarine systems (Rosentreter et al., 2018). In the past decade, methods have been developed to improve the spatial and temporal resolutions of CH₄ concentration and flux measurements in aquatic systems. For example, using real-time in situ measurements based on a gas equilibrator coupled to cavity ring-down spectroscopy (CRDS), Call et al. (2015) and (2019) showed variability across days to weeks and Rosentreter et al. (2018) documented seasonal CH₄ variability in mangrove creeks. These high-resolution efforts have facilitated an improved understanding of different pathways, sources, and sinks in mangrove forests, yet the amplitude and underlying mechanisms of this variability in other coastal marine ecosystems are largely unknown. In addition, seasonal sampling becomes especially important for annual estimates from underrepresented northern temperate and high-latitude regions, but time-series measurements are often discontinued in winter due to harsh weather conditions.

Although high-resolution measurements are critical for reliably capturing the magnitude of the coastal CH₄ variability, these sampling campaigns can be time-consuming and expensive. As such, it is desirable to determine the sampling effort required to obtain a high-accuracy, representative mean dissolved CH₄ concentration for various coastal environments.

We explored the spatial and temporal variability of CH₄ across various heterogeneous coastal environments by systematically measuring CH₄ concentrations in three widely distributed yet understudied northern temperate coastal habitats (Figure 1a). The

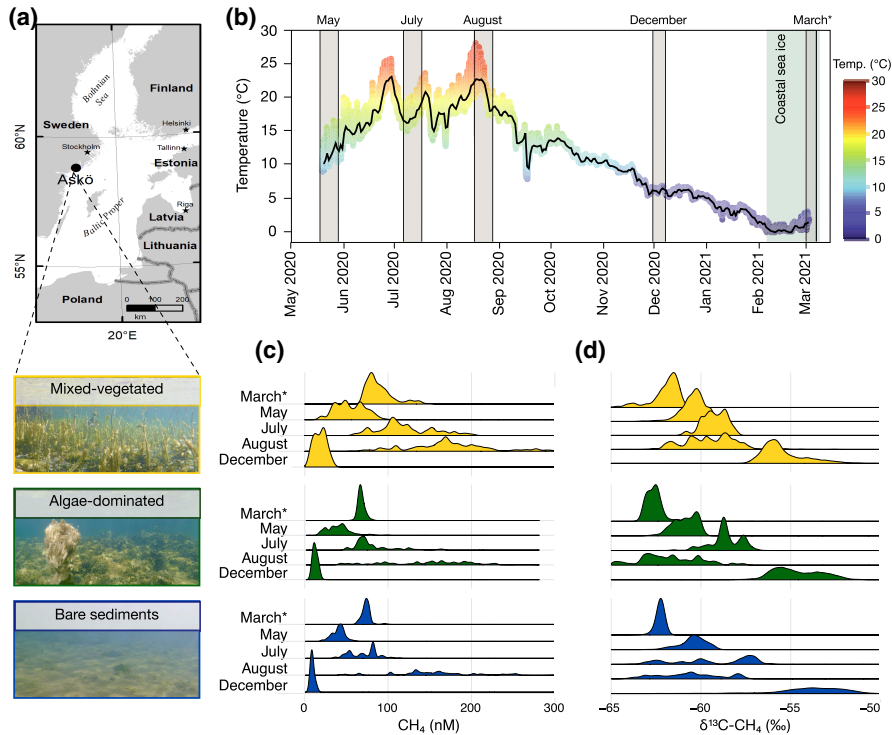


FIGURE 1 Study location and habitat types (a), surface water temperature at the study location (b) and histograms of the density distributions of surface water methane (CH_4) concentrations (c) and stable carbon isotopes of CH_4 (d) across habitats and different sampling months. The five sampling campaigns are depicted as grey bars in (b); the light blue bar indicates the period of coastal sea ice cover. Temperature-coded points are individual measurements at 15 min intervals, and the black line denotes the daily running mean temperature. CH_4 concentrations in (c) >300 nM, which represent $<1\%$ of the data, were omitted for graphical representation but can be found in Table 1. The asterisk denotes under-ice sampling in March

CH_4 distribution in shallow (<4 m water depth) mixed-vegetated, algae-dominated, and adjacent bare sediment habitats was assessed during five sampling campaigns spanning an entire year (Figure 1b), including an ice-covered period in late winter/early spring. We performed in situ real-time monitoring of CH_4 concentrations using CRDS to account for the temporal variability by diel cycles and peak events (Call et al., 2015; Maher et al., 2013; Rosentreter et al., 2018). This state-of-the-art technique also permits high temporal resolution measurements of stable carbon isotope ratios of CH_4 ($\delta^{13}\text{C}-\text{CH}_4$) that help elucidate the controls and formation and removal pathways of the coastal carbon cycle (Maher et al., 2015). All measurements were complemented with benthic vegetation and physicochemical data to (a) provide spatially and temporally resolved CH_4 distribution and emission data from major northern temperate nearshore benthic environments; (b) identify potential biotic and abiotic drivers in shaping the temporal variability of CH_4 ; and (c) test whether current methods are sufficient in resolving the CH_4 distribution within highly heterogeneous and dynamic coastal settings both spatially and temporally.

2 | MATERIALS AND METHODS

2.1 | Study area

This study compares three distinct nearshore shallow (<4 m water depth) coastal habitats located on the island of Askö in the Baltic Sea ($58^{\circ}49'15.4''\text{N}$ $17^{\circ}38'08.8''\text{E}$). The habitats are representative for globally pervasive coastal ecosystems and were identified according to their dominant type of substrate and vegetation: (1)

Mixed-vegetated communities of vascular plants and algae on sediments (hereafter “mixed-vegetated” habitat); (2) mixed turf- and macroalgae on rocks with pockets of sediments (hereafter “algae-dominated” habitat), and (3) surrounding soft sediments without major macrovegetation cover (hereafter “bare sediments”). Each habitat was assessed visually, and the percent cover of the underlying substrate and macrovegetation was recorded within a 5-m radius. Taxa that could not be identified underwater were sampled and confirmed in the laboratory. Benthic surveys were repeated in April and September 2020. Overall, the mixed-vegetated habitat was characterized by coarse sediments with 60–90% total vegetation cover. The vegetation was dominated in equal parts by vascular plants (e.g., *Phragmites australis*, *Stuckenia pectinata*, and *Ruppia spiralis*) and benthic algae (e.g., *Chara aspera* and heterogeneous assemblages of filamentous algae). The “algae-dominated” habitat was situated on rocks and boulders with pockets of permeable sediments with 80–95% total vegetation cover comprised of the macroalgae *Fucus vesiculosus*, and *Ulva* spp., the encrusting *Hildenbrandia rubra*, and various filamentous algae. No vascular plants were identified in this habitat. The surrounding bare sediment habitat with fine soft sediments had 7–10% total vegetation, of which were mainly dislodged *F. vesiculosus* and filamentous algae. The study was conducted at the SW facing side of the island, which is dominated by rocky cliffs and shallow embayments and is relatively open to the Baltic Sea. The habitats were fully submerged at all times due to the absence of tides in this region of the Baltic Sea (Medvedev et al., 2016). The average of measured salinities (i.e., per sampling period and habitat) in the studied area ranged from 6.2 to 7.0 over the course of the year, and, thus, reflected brackish water conditions typical for the central Baltic Sea.

While the Baltic Sea receives freshwater inflows from land and has limited saltwater inflows from the Danish straits, locally at the study site on the island in the outer Stockholm archipelago, there were no major freshwater inputs from rivers or streams, which is reflected by relatively constant salinity throughout the measurement period.

2.2 | Experimental design

We quantified the partial pressures of surface water and atmospheric CH₄ and CO₂ along with the related C-isotopes (i.e., δ¹³C-CH₄ and δ¹³C-CO₂, respectively) in the three habitats during five measurement periods in 2020 and 2021 (i.e., May 18–29; July 6–17; August 17–29; November 30 to December 8, 2020; March 1–6, 2021). For the measurements, we used an adapted version of the Water Equilibration Gas Analyzer System (WEGAS) (details in Humborg et al., 2019) coupled to a CRDS. The system consists of four major components: (i) a submersible seawater intake pump at around 0.3 m water depth mounted to a movable raft that can be deployed noninvasively over the various habitats; (ii) a water handling system comprised of a showerhead equilibrator (1 L headspace volume) and a thermosalinograph (Seabird TSG 45) fed via a hose by the seawater intake pump; (iii) a gas handling system with circulation pumps for the showerhead and ambient air; and (iv) the CRDS gas analyzer for CH₄ and CO₂ concentration and related C-isotope measurements (model G2201-i, Picarro Inc.). The use of a large seawater intake pump results in the combined measurement of CH₄ from ebullition (bubbles) and the dissolved form in the water. The individual contribution of the two forms can, however, not be resolved using the current system. For CH₄ and CO₂ analyses, gas in the showerhead of the equilibrator was measured for 35 min, followed by gas measurements of ambient air for 10 min (i.e., one complete cycle was 45 min). These measurement cycles (i.e., 35 min, water; and 10 min, air measurements) ran continuously during the five measurement periods mentioned above. The raft with the water intake pump was moved between the defined habitats every 24 h from the shore with ropes. Measurements in March were distinct from the other sampling periods due to the ice cover that had been present for 4–6 weeks prior to the time of sampling. Here, holes were drilled into the ice and the pump lowered to measure “under-ice” concentrations. We validated the CRDS analyzer's performance according to the manufacturer's instructions with “ALPHAGAZ™ Stable Isotope Ratio Gases” for Picarro instruments. Specifically, before each deployment period, we injected three standards with varying CO₂ and CH₄ bulk concentrations, and varying δ¹³C-CO₂ and δ¹³C-CH₄ isotope values (i.e., low = 1.00 ppm CH₄, -24.20‰ δ¹³C-CH₄, 250.00 ppm CO₂, -5.00‰ δ¹³C-CO₂; natural = 1.77 ppm CH₄, -48.30‰ δ¹³C-CH₄, 399.00 ppm CO₂, -8.50‰ δ¹³C-CO₂; and high = 10.00 ppm CH₄, -68.60‰ δ¹³C-CH₄, 1000.00 ppm CO₂, -20.10‰ δ¹³C-CO₂). Measurements with each standard ran for 10 min, and three-point calibration lines were constructed whose regression coefficients were used to scale the unknown sample data if needed.

Concentration and isotope measurement at 1 Hz frequency were averaged and logged every 10 s. The recorded data were filtered by removing data from the transition period between ambient air and water measurements due to the response time of CRDS to sharp changes in concentrations of CH₄ and CO₂. Data were also removed during improper functioning (e.g., low water flow). For this study, we used 210,059 (averaged from 2,100,590 measurements at 1 Hz) data points each for CH₄, CO₂, δ¹³C-CH₄, and δ¹³C-CO₂ for statistical purposes. CH₄ concentrations in water (in ppm obtained by the CRDS) were converted to molar concentrations (i.e., CH₄ in nM) and CO₂ was converted to pressure units (i.e., pCO₂ in μatm) (Humborg et al., 2019). Alongside CRDS measurements, several other environmental and meteorological variables were recorded. Surface water temperature, pH, and dissolved oxygen concentrations at the point of water intake were logged every 15 min using a multiparameter sonde (model EXO2, YSI) that was calibrated prior to each deployment. Water temperature and salinity were also recorded with every CRDS measurement with a thermosalinograph (Seabird TSG 45) that was positioned before the showerhead equilibrator. Wind data observations (wind speed and direction) and air temperature were obtained from a Metek uSonic-3 heated 3D sonic anemometer, and a Vaisala HMP155 shielded temperature probe mounted on a 1.5-m high meteorological mast. The mast was located at the waterline in a coastal bay, approximately 400 m to the northwest of the sampled habitats. Mean winds were adjusted to a 10-m reference height assuming a logarithmic profile with neutral stability (Haugen, 1973):

$$U_{10} = U + \left(\frac{u^*}{\kappa}\right) \times \log\left(\frac{10}{z_u}\right)$$

where U is the measured wind speed at height z_u , u^* is the measured friction velocity by the 3D sonic anemometer, and κ is the von Karman constant (0.4).

2.3 | Exploration of the CH₄ distribution variability

We used a generalized linear model (GLM) to examine differences across habitats within each month. Due to positive-skewed data and overdispersion, a quasi-Poisson model was constructed using the `glm()` function in R (R Core Team, 2021) with “Month” (i.e., March, May, July, August, December) and “Habitat” (i.e., Mixed-vegetated, Algae-dominated, and Bare sediments) as factors. We used the R package “EMMEANS” (Lenth et al., 2019) for pairwise post hoc multiple comparisons with Bonferroni-adjusted p-values. Results and model details are presented in Table S1. The relationships among CRDS and environmental data were initially assessed using principal component analysis (PCA) using the R packages “FACTOMINER” (Husson et al., 2016) and “FACTOEXTRA” (Kassambara & Mundt, 2017). PCA is a multivariate technique used to emphasize variation and to visualize patterns in a dataset, particularly when there are many variables. Upon the visual inspection of the PCA, we calculated Spearman coefficients for correlations between

TABLE 1 Methane (CH₄) concentrations and saturations in the three studied nearshore coastal habitats

Month	Habitat	CH ₄ (nM)				CH ₄ saturation (%)	
		Mean (±SD)	CV (%)	Median (IQR)	Range	Median (IQR)	N
March*	Mixed-vegetated	90 (±17)	19	84 (78–96)	68–152	1659 (1530–1892)	6904
	Algae-dominated	68 (±4)	6	67 (66–70)	57–82	1320 (1289–1371)	4495
	Bare sediments	74 (±5)	7	74 (71–76)	60–102	1438 (1389–1493)	6083
May	Mixed-vegetated	56 (±17)	30	56 (42–69)	17–103	1369 (1034–1672)	19,573
	Algae-dominated	41 (±15)	37	40 (27–49)	17–101	980 (731–1159)	17,894
	Bare sediments	40 (±8)	20	41 (35–45)	20–75	980 (908–1071)	18,056
July	Mixed-vegetated	119 (±33)	28	112 (99–144)	58–204	3056 (2720–4059)	7182
	Algae-dominated	80 (±24)	30	71 (66–85)	45–169	1949 (1800–2335)	10,885
	Bare sediments	69 (±17)	25	70 (54–82)	34–115	1977 (1517–2249)	11,961
August	Mixed-vegetated	190 (±74)	39	174 (150–211)	53–460	5275 (4624–6563)	21,801
	Algae-dominated	144 (±54)	38	153 (97–189)	41–274	4755 (2847–5850)	23,597
	Bare sediments	161 (±53)	33	151 (133–185)	41–324	4570 (3991–5835)	19,210
December	Mixed-vegetated	18 (±7)	39	19 (12–24)	6–37	426 (258–526)	17,253
	Algae-dominated	13 (±3)	23	12 (11–15)	9–23	252 (230–332)	11,878
	Bare sediments	9 (±2)	22	9 (8–10)	6–17	191 (163–214)	10,587
Annual	Mixed-vegetated	97 (±79)	81	77 (34–143)	6–460	1707 (849–4287)	75,413
	Algae-dominated	79 (±61)	77	65 (32–116)	9–274	1508 (803–3250)	68,749
	Bare sediments	79 (±64)	81	57 (38–122)	6–324	1424 (937–3690)	65,897

The saturation of CH₄ is relative to the dissolved equilibrium with ambient air.

Abbreviations: CV, coefficient of variation; IQR, interquartile range; N, number of individual observations (10 s average of 1 Hz measurements); SD, standard deviation. The asterisk denotes under-ice sampling in March.

surface water CH₄ concentration and potential environmental drivers (i.e., water temperature, salinity, dissolved oxygen and CO₂ concentrations, and pH).

The thermal sensitivity of the CH₄ distribution was further explored by applying principles of the metabolic theory of ecology (MTE) (Sibly et al., 2012), calculating the activation energy (E_a) based on Arrhenius equations in the seasonal thermal regime. The activation energies (E_a in eV) were estimated by fitting a linear regression equation between the natural logarithm of CH₄ concentrations and the reciprocal of temperature ($1/kT$), where k is the Boltzmann's constant (8.62×10^{-5} eV K⁻¹) and T is the measured water temperature in Kelvin. E_a s allow for a comparison of temperature dependencies across systems and metabolic processes (Sibly et al., 2012).

We applied the Rayleigh model to estimate the fraction of CH₄ that was oxidized in surface water in each habitat and sampling month, as:

$$\delta^{13}\text{C}_{\text{CH}_4}(\text{CRDS}) = \delta^{13}\text{C}_{\text{CH}_4}(\text{S}) + \epsilon(\text{Inf})$$

where $\delta^{13}\text{C}_{\text{CH}_4}(\text{CRDS})$ is the isotopic composition of surface water CH₄ measured with the CRDS system, $\delta^{13}\text{C}_{\text{CH}_4}(\text{S})$ is the isotopic value of the CH₄ source in sediments, -67% that has been measured in local sediments, ϵ is the isotope fractionation factor for CH₄ oxidation of -20% (Bastviken et al., 2002), and f represents the fraction of remaining CH₄ in surface water, that is, $1-f$ is the

fraction of oxidized CH₄. The Rayleigh model assumes a closed system when CH₄ oxidation occurs, which means CH₄ oxidation is the only sink of CH₄ in water column and is faster than the refreshment of CH₄ supplied to the surface water. This is an oversimplification given the high variability of coastal systems. The true fraction of CH₄ oxidized in surface water could, thus, be underestimated due to the contribution of ¹³C-depleted CH₄ source mixing with surface water CH₄ with higher $\delta^{13}\text{C}_{\text{CH}_4}$ values in a partially open system.

2.4 | Sampling effort evaluation of dissolved CH₄ concentrations

We used a bootstrapping exercise to determine the minimum number of concentration measurements per day required to obtain a high-accuracy, representative daily mean dissolved CH₄ concentration across the various coastal habitats and sampling months. The assumption of these simulations is that our high-resolution sampling effort (i.e., one sample per second) can sufficiently capture the temporal variations of surface water CH₄ concentrations for each habitat. We randomly sampled the population of measured CH₄ concentrations assuming a variable sample size, from 1 to 600 samples a day (with sample replacement). This sampling was repeated 200 times for each sample size, and for each simulation, we calculated the resulting mean CH₄ concentration.

2.5 | Sea-air flux computation

The sea-air flux (F) of CH_4 was calculated as:

$$F = k \times K_0 \times (p\text{CH}_{4\text{sea}} - p\text{CH}_{4\text{air}})$$

where k (m s^{-1}) is the gas transfer velocity, K_0 ($\text{mol m}^{-3} \text{atm}^{-1}$) is the aqueous-phase solubility of CH_4 , and $p\text{CH}_{4\text{sea}}$ and $p\text{CH}_{4\text{air}}$ are the measured partial pressures (atm) of CH_4 in the near-surface water and in the air, respectively. We compared our site-specific atmospheric CH_4 concentration measurements to data of the closest ICOS atmospheric monitoring station (i.e., Utö-Baltic Sea station; station ID: UTO). Locally measured $p\text{CH}_4$ ranged from 1.884 to 2.124 (mean \pm SE = 1.969 ± 0.063) over the study period, which compares to 1.921–2.112 (mean \pm SE = 1.978 ± 0.001) from the ICOS Utö-Baltic Sea station (Laurila, 2021). Despite similar mean values over the study period, locally measured $p\text{CH}_4$ reflects better the site-specific variability and is, thus, more suitable for the computation of air-sea fluxes, especially if concentration gradients (i.e., water to atmosphere) are small. The solubility is determined from Wiesenburg and Guinasso (1979) as:

$$\ln \beta = A1 + A2(100/T) + A3 \ln(T/100) + S [B1 + B2(T/100) + B3(T/100)^2]$$

where β is the dimensionless (mL of gas dissolved per mL of H_2O) Bunsen solubility coefficient, $A1$, $A2$, $A3$, and $B1$, $B2$, $B3$ are constants from Table 1 in Wiesenburg and Guinasso (1979), T is the measured water temperature (K), and S the measured salinity (‰). Assuming CH_4 behaves as an ideal gas, K_0 is related to β by $K_0 = \beta (R \times T_{\text{STD}})^{-1}$, where R ($\text{m}^3 \text{atm K}^{-1} \text{mol}^{-1}$) is the ideal gas constant and T_{STD} (K) is the standard temperature in Kelvin.

The gas transfer velocity (k) used is that determined by Wanninkhof (2014) as:

$$k = 0.251 \times U^2 \times \left(\frac{Sc_{\text{balticsea}}}{660} \right)^{-0.5}$$

where U is the wind speed (m s^{-1}) at 10 m height and $Sc_{\text{balticsea}}$ is the Schmidt number at the measurement site, which is dependent on temperature, salinity, and gas molecule. Sc was corrected for the corresponding temperature that was measured simultaneously with partial pressures of CH_4 ($p\text{CH}_4$) according to coefficients taken from Table 1 in Wanninkhof (2014). Furthermore, the Schmidt number for Baltic Sea brackish water (i.e., $Sc_{\text{balticsea}}$) with measured salinity ($S_{\text{balticsea}}$) was calculated by interpolation of Sc for fresh water (salinity 0‰) and sea-water (salinity 35‰) following (Gülzow et al. 2013) and (Jähne et al. 1987):

$$Sc_{\text{balticsea}} = \frac{(Sc_{\text{seawater}} - Sc_{\text{freshwater}}) \times S_{\text{balticsea}}}{35} + Sc_{\text{freshwater}}$$

All fluxes are expressed in $\mu\text{mol CH}_4 \text{m}^{-2} \text{day}^{-1}$. Other variables (e.g., currents, waves, water depth) can also be used to predict k in

coastal environments, but the studied location does not have any significant permanent or tidal currents, and estuarine models may not provide better results for our setting. Furthermore, Lundevall-Zara et al. (2021) tested other wind-based k models in similar habitats of the same location and concluded that calculated average k -values from different models were close to those of the Wanninkhof (2014) relationship for the range of wind velocities encountered on the island of Askö. Thus, for a better comparability across studies, we have therefore decided to use this relationship.

2.6 | Estimating annual sea-air fluxes of CH_4

We estimated sea-air fluxes of CH_4 across all habitats over the entire annual cycle. Based on the strong temperature dependencies of CH_4 concentrations, we calculated CH_4 concentrations outside of the measurement periods using the Arrhenius equations from Figure 3b and the 15-min interval surface water temperature measurements from March 3, 2020 to March 3, 2021 (Figure 1b), as:

$$\ln \text{CH}_4 (\text{nM}) = a + b * \left(\frac{1}{kT} \right)$$

with $\ln \text{CH}_4$ as the natural logarithm of the CH_4 concentration in nM, a and b as intercept and slope, respectively, and the reciprocal of temperature ($1/kT$), where k is the Boltzmann's constant ($8.62 \times 10^{-5} \text{ eV K}^{-1}$) and T is the measured water temperature in Kelvin. For the mixed-vegetated, algae-dominated, and the bare sediment habitat, the intercepts were 47.14, 47.36, and 51.66, respectively, and the slopes were -1.02 , -1.03 , and -1.13 , respectively.

We determined the difference between the measured and the estimated CH_4 concentrations per habitat and month (where measured data were available) as the percentage of the calculated value (i.e., the percent error). Overall, there was a good agreement of the temperature-based calculated CH_4 concentrations with the actual measured concentrations across all habitats in May, July, and August (i.e.; mostly $<10\%$ deviation of the means; Table S2). Calculated CH_4 concentrations in March and December tended to be underestimated by 20–50% relative to the measured concentrations. The data show that temperature can be a good proxy to estimated CH_4 concentrations if enough in situ data are available. However, it also becomes apparent that, when absolute concentrations are low, disparities of few nanomole in the CH_4 concentration likely contributed to large differences (Table S2).

Sea-air fluxes of CH_4 were then calculated based on equations provided above, assuming an average salinity of 6.6 (i.e., the average of measured salinities ranging from 6.2 to 7.0 over the course of the year). Wind speed data from the study location matching the CH_4 concentrations (measured and calculated) was available for 21,445 out of 34,932 data points (61%). The remaining wind speed data were estimated using a Monte-Carlo simulation on the distribution (mean \pm SD, $2.25 \pm 2.01 \text{ m/s}$) of available wind speed data from that year.

3 | RESULTS

3.1 | CH₄ concentrations and δ¹³C-CH₄ values across coastal habitats

We report a high spatial and temporal variability of surface water CH₄ concentrations across the mixed-vegetated, algae-dominated, and bare sediment habitats that span two orders of magnitude, ranging from 6 to 460 nM (Figure 1c; Table 1). During all sampling periods, the highest concentrations were always observed in the mixed-vegetated habitat, followed by algae-dominated, and surrounding bare sediment habitats (Table 1). A generalized linear model (GLM) with pairwise post hoc multiple comparisons confirmed that CH₄ concentrations differed significantly across habitats within each sampling month (Table S1), with an exception of the algae-dominated and bare sediment habitats in May. In addition, differences between the algae-dominated and bare sediment habitats were minor (expressed by odds ratios close to 1 as effect size statistics) in May, July, and August (Table S1). There were strong seasonal variations of CH₄ concentrations with similar patterns across all habitat types. In general, the highest CH₄ concentrations were observed in August, followed by July, March, May, and December (Figure 1c; Table 1). The δ¹³C-CH₄ values of surface water varied by >7‰ over the sampling months in all habitat types. Across all habitats, CH₄ was most enriched in ¹³C in December (average of -55‰) and became most depleted in March, approaching -63‰ (Figure 1d). Differences in δ¹³C-CH₄ values across habitats in the same month occurred only in some cases and were smaller than the annual temporal variation (Table S3).

CH₄ concentrations also varied greatly during each sampling month and in each habitat type (Figure 1c). Most variability within months was ascribed to CH₄ concentration changes independent of the time of the day (Figure 2a-c). "Peak events" with >100% change of the CH₄ concentrations occurred within hours and were observed in all habitats and during all sampling campaigns (Figure 2d-f). We used the coefficient of variation (CV) as a standardized measure that describes the dispersion of the CH₄ distribution around the mean to quantify and compare the within-month variability. Overall, the CVs ranged from 5% to 39%, with the lowest variability of CH₄ concentrations in March when the surface water was covered with ice and the highest variability generally occurring in July and August (Table 1). An exception to the seemingly random CH₄ variability within one diel cycle was the mixed-vegetated habitat in August, when CH₄ consistently peaked during midday (mean ± SD, 333 ± 93 nM at 13:00 h local time), and was lowest at night (141 ± 24 nM at 02:00 h local time; Figure 2a).

3.2 | Correlation of surface water CH₄ with environmental variables

Principal component analysis (PCA) revealed distinct separation of the CH₄ and environmental data across months and to a lesser extent across habitats (Figure 3a). The first two principal components

explained 43.2% of the variation in the data. Separation was greatest along principal component axis 1 (PC1 = 24.6%) that split the groups into five distinct clusters representing the sampling months March, May, July, August, and December. Variations in CH₄ concentrations (32.1%), temperature (23.4%), salinity (14.8%), and oxygen (11.0%) contributed most to the separation of the data along principal component axis 1. Data points within each month spread predominantly along principal component axis 2 (PC2 = 18.46%), and their variation was driven by the time of the day, CO₂ concentrations, and pH.

Upon the visual inspection of the PCA (Figure 3a), we computed correlation matrices based on Spearman's rank correlation coefficient of CH₄ concentrations in each habitat with temperature, salinity, CO₂, O₂, and pH (Figure S1). Temperature showed the

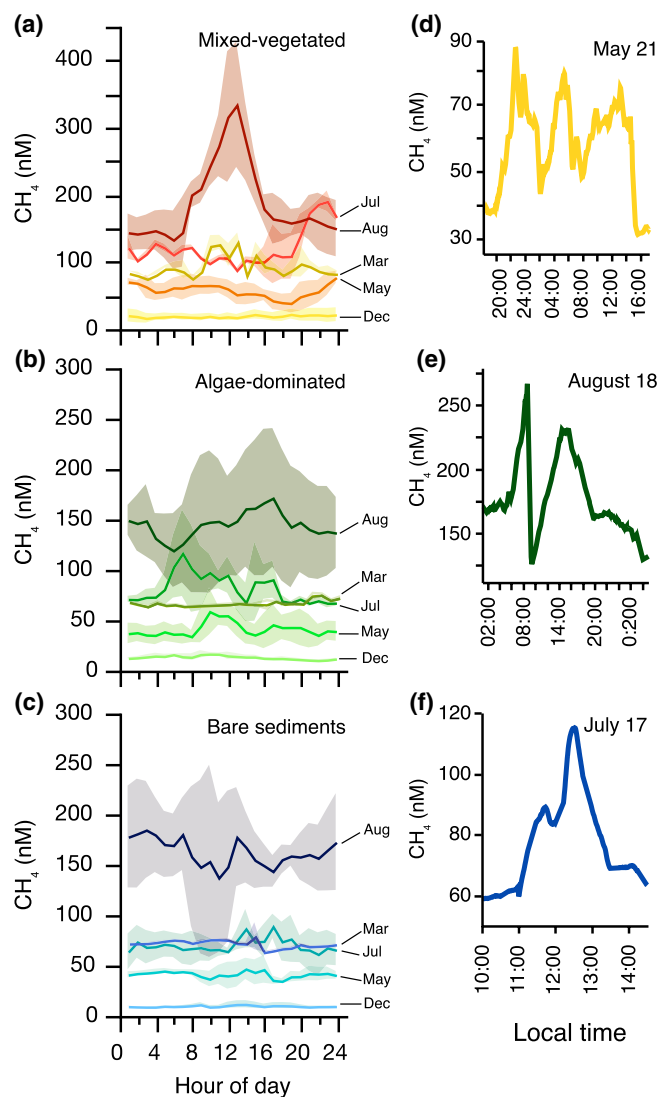


FIGURE 2 Mean of hourly CH₄ concentrations over full diel cycles in mixed-vegetated (a), algae-dominated (b), and bare sediment (c) habitats during various sampling months, and exemplary CH₄ concentration peaks ('peak events') of continuous (1 Hz) data in the respective habitats (d-f). Shaded areas in (a-c) depict the standard deviation around the mean derived from multiple days of measurements within the same month. Note the different scales on the y-axes

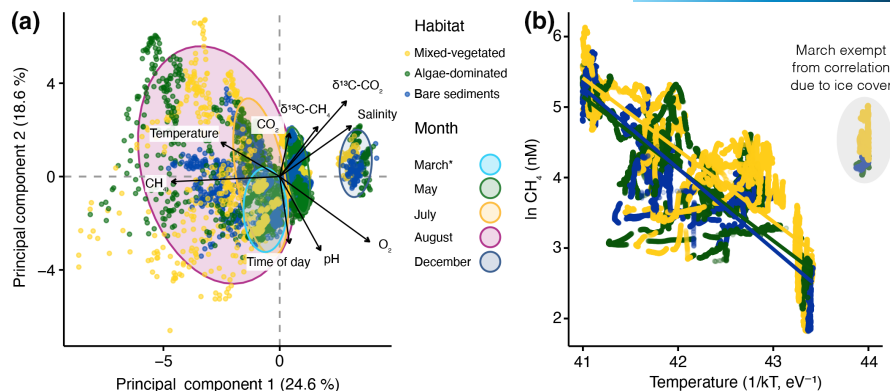


FIGURE 3 Principal component analysis (PCA) using all environmental data (a) and Arrhenius plot showing the relationship between the inverted temperature multiplied by the Boltzmann constant ($1/kT$) and the natural logarithm of the CH_4 concentrations (b) from mixed-vegetated, algae-dominated, and bare sediment habitats. PCA allows the variables to be projected in multidimensional space to highlight the relationships between them. The vectors represent the individual environmental variables. When vectors are far from the center and close to each other, they are positively correlated, whereas when they are symmetrically opposed, they are negatively correlated. If the arrows are orthogonal, they are not correlated. Overall, 43.2% of the total variation is explained by the first two axes, 24.6% and 18.6%, respectively. Solid colored lines in (b) indicate the linear regression (details in the text). CH_4 = surface water methane concentrations; CO_2 = surface water carbon dioxide concentrations; O_2 = surface water dissolved oxygen concentrations. The asterisk denotes under-ice sampling in March. We excluded data points encircled in (b) from the linear regression due to ice cover in March and the resulting irregular response to temperature

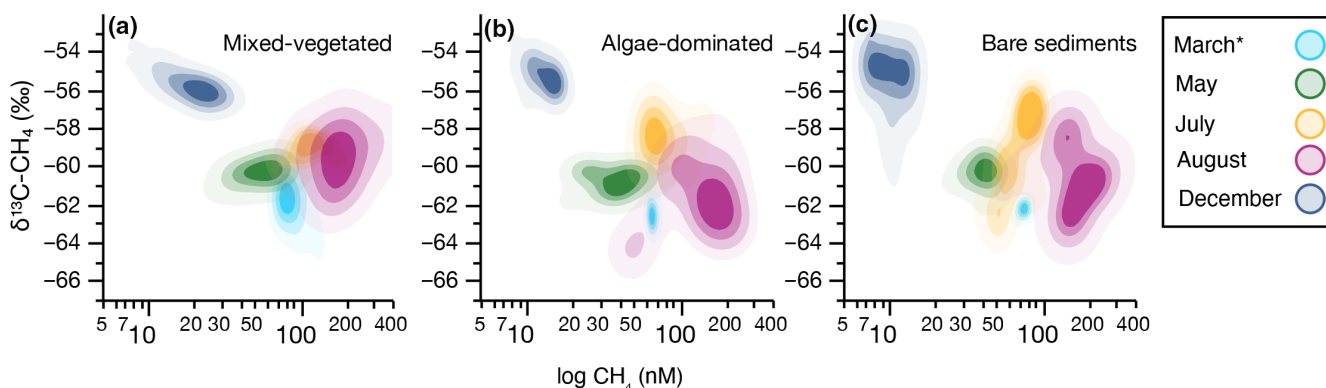


FIGURE 4 Stable carbon isotopes of methane ($\delta^{13}\text{C-CH}_4$) as a function of the $\log \text{CH}_4$ concentrations of surface water in three shallow coastal habitats (a–c) of the Baltic Sea. The data is represented as a nonparametric bivariate surface to describe the density of all data pairs ($n = 210,059$ in total). The contour lines are quantile contours in 20% intervals. The asterisk denotes under-ice sampling in March

strongest positive association with CH_4 concentrations in the algae-dominated habitat ($r^2(68,740) = .82$, $p < .0001$), followed by bare sediments ($r^2(65,812) = 0.71$, $p < .0001$), and the mixed-vegetated habitat ($r^2(75,410) = 0.70$, $p < .0001$). Weaker and negative associations were also apparent for O_2 , CO_2 , and salinity in all habitat types (Figure S1). pH was negatively associated with CH_4 concentrations in the mixed-vegetated and algae-dominated habitat but positively in the surrounding bare sediments. Given the strong association with temperature, we further explored the thermal sensitivity of the CH_4 distribution by calculating the apparent activation energy (E_a in eV) based on Arrhenius equations in each habitat within the seasonal thermal regime (Figure 1b). Estimated E_a s were similar across all habitats with positive (i.e., higher CH_4 concentrations at higher temperature) values of 1.13 eV ($F(1,59,812) = 277,552.7$, $p < .0001$, $r^2 = .82$) in bare sediments, 1.03 eV ($F(1,64,252) = 256,516.8$, $p < .0001$, $r^2 = .80$) in algae-dominated, and 1.02 eV ($F(1,65,807) = 204,754.7$,

$p < .0001$, $r^2 = .80$) in the mixed-vegetated habitat, respectively (Figure 3b).

The $\delta^{13}\text{C-CH}_4$ signatures provided an additional dimension to reveal the main processes controlling CH_4 variability given the isotope fractionation associated with CH_4 production and consumption (i.e., oxidation) (Barker & Fritz, 1981). $\delta^{13}\text{C-CH}_4$ values as a function of CH_4 concentrations reflected temporal variations across seasons (Figure 4). In all habitats, the lowest CH_4 concentrations with the highest $\delta^{13}\text{C-CH}_4$ values were observed in December, while the highest CH_4 concentrations and the lowest $\delta^{13}\text{C-CH}_4$ values were found in August and March. The Rayleigh model, assuming that the supply of CH_4 is much slower than oxidation in water column, was applied to estimate the fraction of CH_4 that was oxidized in surface water, suggesting 20% of CH_4 loss through oxidation in August and March, and up to 50% in December in all habitats (Table S3).

3.3 | Sea-air fluxes of CH₄

Surface waters were supersaturated throughout all measurement periods and habitats relative to CH₄ in ambient air. The median (IQR) CH₄ saturation in the mixed-vegetated habitat was 1706 (848–4286)%, 1508 (802–3250)% in algae-dominated, and 1423 (937–3689)% in adjacent bare sediment habitats. The resulting sea-air flux rates of CH₄ were highly variable and ranged from 0.1 to 3852 μmol CH₄ m⁻² day⁻¹ during ice-free periods and primarily reflected differences in water column CH₄ concentrations between habitats and months (Table S4). The median (IQR) CH₄ flux rates were highest during measurement periods in July, with 138 (81–245), 98 (26–172), and 77 (36–119) μmol CH₄ m⁻² day⁻¹ in the mixed-vegetated, algae-dominated, and bare sediment habitat, respectively. The high CH₄ flux rates in July coincided with high wind speeds during this month (Table S4). CH₄ flux rates were lowest in all habitats in December, with median values of 0.7–3.5 μmol CH₄ m⁻² day⁻¹. No fluxes were computed for the ice-covered period. The estimated annual median (IQR) sea-air fluxes were 12 (3–43), 10 (2–32), and 7 (2–29) μmol CH₄ m⁻² day⁻¹ in the mixed-vegetated, algae-dominated, and bare sediment habitat, respectively.

4 | DISCUSSION

Our high-resolution measurements revealed differences in the distribution of surface water CH₄ concentrations across neighboring coastal habitats over short spatial (within meters) scales and exceptionally high temporal variability that could only be detected with continuous measurement techniques during several seasons. Acknowledging this high spatiotemporal variability is critical to confine CH₄ emissions from coastal environments and the variability associated with their habitat heterogeneity.

4.1 | Temperature sensitivity of coastal CH₄ distribution

Median CH₄ concentrations measured across the here-studied habitats were 4–13 times higher than those observed in deeper waters of the open Baltic Sea (Schmale et al., 2010; Wilson et al., 2018), up to three times higher than previously published data for coastal Baltic areas (Humborg et al., 2019; Ma et al., 2020), and substantially higher than globally compiled nearshore CH₄ concentrations (Weber et al., 2019) (Table S5). The magnitude highlights that vegetated coastal ecosystem are characterized by excessive organic matter loads from primary production, trapping and accumulation of allochthonous organic matter, and sedimentary conditions that can favor CH₄ production (Dale et al., 2019; Wallenius et al., 2021). However, we also report an exceptionally high spatiotemporal variability of surface water CH₄ concentrations.

A first major source of this variability was attributed to seasonal differences in CH₄ concentrations. The significant correlation

between CH₄ concentrations and temperature over the sampling months suggests that temperature mainly regulates seasonal variations. Like most other forms of metabolism, methanogenesis is temperature-dependent, and the calculated apparent activation energies ($EA = -1$ eV, across all habitats) were in line with previous global estimates of ecosystem-scale CH₄ fluxes with an EA of 0.96 eV (Yvon-Durocher et al., 2014). Thus, the higher CH₄ concentrations in late summer are likely due to increased production under warmer water temperatures. Historical data from the nearby oceanographic observation station “2507 Landsort Norra” between 2010 and 2020 confirmed that the annual surface water temperature curve from our study area is representative of previous years (Sveriges meteorologiska och hydrologiska institut, 2022). We infer that the observed temperature sensitivity is primarily driven by natural temperature variations rather than a warming effect. Both aerobic CH₄ oxidation together with anaerobic CH₄ oxidation in sediments may also increase in summer due to temperature controlling their rates (Treude et al., 2005; Zehnder & Brock, 1980) and the increased supply of CH₄ supply by molecular diffusion. However, in summer, the overall production of sedimentary CH₄ likely outweighed the relative contribution CH₄ oxidation pathways. In support of this, parallel measured δ¹³C-CH₄ values combined with the Rayleigh model revealed that the relative contribution of CH₄ production versus oxidation shifted across seasons. CH₄ oxidizing bacteria favor isotopically lighter CH₄, leaving the residual CH₄ with heavier isotopes. Low CH₄ concentrations accompanied by high δ¹³C-CH₄ values suggest that up to 50% of CH₄ was oxidized in winter, indicating an important role of CH₄ oxidation in removing CH₄ relative to CH₄ production. This microbial oxidation efficiency decreased to 20–30% in summer due to a boosted supply of CH₄ to the water column relative to its oxidation. High oxygen concentrations mediated by the photosynthetic activity of algae and plant communities during the day and increased light exposure in summer may have contributed to inhibiting CH₄ oxidation (Murse & Sugimoto, 2005; Rudd et al., 1976).

4.2 | Ice-cover effects on CH₄ dynamics

An exception to the overall seasonal trend was observed in March (i.e., late winter/early spring). Measurements during this month were marked by ice cover that, to this point, had been present for 4–6 weeks. Analogous to many northern lakes (Denfeld et al., 2018), we observed an accumulation of CH₄ under the ice, with mean concentrations six times higher than in December (last month without ice cover). More negative δ¹³C-CH₄ values in March (–62 to –64‰) suggest CH₄ supply with overall low oxidation. This observation corroborates studies showing suppressed methanotrophic activity at very cold temperatures (e.g., Phelps et al., 1998). Calculations of the Rayleigh model confirmed that <20% of the surface water CH₄ was oxidized during this period. However, the CH₄ depleted in ¹³C could also be a result of varying fractionation during methanogenesis at lower temperatures or mixed CH₄ formation pathways. The CH₄ accumulation under ice will likely result in enhanced outgassing events

following ice break (Ducharme-Riel et al., 2015; Karlsson et al., 2013). Whereas under-ice CH₄ accumulation is a well-studied feature of northern lakes, these dynamics have not been described for northern temperate coastal regions with regular sea ice every year. Our data suggest the necessity to include the ice-covered period and CH₄ outgassing during ice breakup in future coastal CH₄ sampling strategies and the annual CH₄ budget of northern temperate and high-latitude regions (Omstedt et al., 2004).

4.3 | Physical forcing may drive short-term CH₄ variability

A second major source of variability in the CH₄ concentrations was short-term variations that occurred within hours (Figure 2d–f). Most of this variability was independent of the time of the day and without an apparent and reoccurring diel pattern. However, fluctuations of the CH₄ concentrations were so strong that the minimum and maximum values within one habitat and sampling campaign (time window max. 12 days) could differ by up to one order of magnitude (Table 1). The dispersion of the CH₄ probability distribution around the mean concentration was on average 30% during the ice-free months and, thus, much higher than the reported global open ocean CH₄ variability with CVs ranging between 2% and 11% (Wilson et al., 2018). While we could not find any direct correlation to the available environmental data, one possible explanation for the high variability could be the physical influence of the open coastal setting through wind and/or wave action. A wave-induced pumping effect on the pore water pressure can transport solutes from deeper to surface layers (Precht & Huettel, 2004; Yang et al., 2019); Thus, varying CH₄ release rates from permeable coastal sediments in very shallow waters may cause variable near-surface CH₄ concentrations, as has been shown relevant even for lake systems (Hofmann et al., 2010). In support of this, the CVs of the CH₄ distribution were much lower across all habitats in March (mean CV = 10%), when, due to ice cover, the influence of waves and winds on the water column and sediments was likely minor and no CH₄ escaped to the atmosphere.

4.4 | Reoccurring diel CH₄ patterns in summer

A reoccurring diel pattern in CH₄ concentration changes was only observed in the mixed-vegetated habitat in August, with the highest concentrations consistently toward midday and lowest at night. This marked diel variation may be attributed to plant-mediated transport of CH₄ by convective throughflow from rooted submerged plants, which were only present in the mixed-vegetated habitat. The convective transport through pressure gradients can account for up to 60% of the total CH₄ transport from sediments during daylight hours and high photosynthetic activity (Kim et al., 1998; van den Berg et al., 2020). In the early stages of plant growth, molecular diffusion through dead/live plants into

the standing water column can be the primary transport mechanism (Kim et al., 2001). Most plants at the mixed-vegetated site were fully submerged; thus, a sediment–plant–water flux is likely. However, *Phragmites* stems (comprising ~10% of the total vegetation in the mixed-vegetated site) possibly facilitated a sediment–plant–air flux of CH₄ (van den Berg et al., 2020), which will have remained undetected with our approach. Abiotic CH₄ photoproduction from organic matter degradation may also play a role in shaping site-specific CH₄ dynamics in oxygenated surface waters (Li et al., 2020; Zhang & Xie, 2015). However, given that reoccurring and pronounced diel cycles were only visible in one of the three neighboring habitats, benthic/plant-mediated pathways seem more likely to have caused the patterns observed. Overall, the contribution of plant-mediated fluxes and the relation to seasonal succession patterns of submerged vegetation, along with the contribution of CH₄ photoproduction in shallow coastal waters with high incident irradiance remain uncertain and need further investigation.

4.5 | Spatial distribution of CH₄ reflects coastal ecosystem mosaic

Shallow coastal habitats are heterogeneous, and the variation in spatial structure and temporal change of benthic communities defines the expression of ecosystem functions in form and magnitude (Snelgrove et al., 2014). Reflecting the coastal ecosystem mosaic (Sheaves, 2009), some of the measurements across the studied neighboring habitats were not further than 30–50 m apart. Yet, despite their proximity, we observed significant differences in the distribution of CH₄ in the water column and the magnitude of the resulting sea–air fluxes. Surface water CH₄ concentrations are likely related to variable CH₄ production and oxidation rates, as indicated by varying δ¹³C-CH₄ values across sites during some months (Figure S3). These differences may be ascribed to different quantities and qualities of organic matter deposited within local sediments and differences of sediment properties (e.g., porosity) (reviewed in Rosentreter et al., 2021a). The presence of rooted vegetation may also play a role in the small-scale variability, as roots provide substrate via root litter and exudates and transport oxygen into the sediments. In addition, while the employed system measures CH₄ in the dissolved form and from ebullition (bubbles), the individual contribution of the two phases cannot be resolved but may contribute to differences between the habitat types. It becomes apparent that more research is required to determine the spatial scale of this variability and to understand better the controls on substrate availability for methanogenesis. In particular, links between biodiversity metrics (i.e., abundance and biomass) of primary and secondary producers and CH₄ production and consumption pathways need to be better constrained as has been shown relevant for seafloor metabolism (i.e., gross primary production and community respiration) in shallow waters (Rodil et al., 2021). Likewise, integrating knowledge on the structure

of sediment microbial communities associated with the different habitats is imperative to improve the prediction of CH_4 production and oxidation pathways from different coastal habitats (Wallenius et al., 2021).

4.6 | High sampling intensity is required to capture coastal CH_4 variability

Particularly the high temporal variability on timescales from hours to days complicates our ability to generalize the distribution of CH_4 in nearshore coastal environments and obstructs efforts to confine diffusive flux calculations that are based on concentration measurements. Therefore, we conducted a bootstrapping analysis on our continuous data to determine the minimum number of individual concentration samples per day required to obtain a high accuracy, representative mean dissolved CH_4 concentrations. The data exploration shows that collecting one discrete water sample a day, a typical approach used to describe CH_4 concentration differences across geolocations (Banerjee et al., 2018; Dutta et al., 2015; Nirmal Rajkumar et al., 2008), results in a large uncertainty, with a potential to over- or underestimate the mean CH_4 concentration by almost 70%. Specifically, taking only one sample per day from the mixed-vegetated habitat in August would result in a mean CH_4 concentration with a 5th–95th percentile of 90–320 nM based on 200 simulations. Increasing the sampling intensity to five samples per day reduces the uncertainty to 30%. In comparison, 50 samples per day instead would narrow this uncertainty to a 5th–95th percentile of 171–209 nM (10% uncertainty), closer to the observed true mean CH_4 concentration of 191 nM during this period (Figure 5a). A similar pattern was apparent in all other habitats and sampling periods (Table S6). Consequently, the data collection and sampling strategy are detrimental to accurately capturing the temporal variability and assure justified mean CH_4 concentrations that are the

basis for flux computations. Thus, near-continuous measurements using CRDS (Hartmann et al., 2018; Humborg et al., 2019; Maher et al., 2013) or similar systems to determine in situ CH_4 concentrations in surface waters are desirable when addressing complex pathways and transformations of CH_4 in coastal ecosystems. For annual estimates, seasonal measurements that reflect local climatological patterns will be required.

4.7 | Northern temperate coastal habitats are seasonal CH_4 emission hotspots

The high-resolution CH_4 concentration measurements allowed us to establish annual CH_4 emission estimates across all habitat types. The diffusive CH_4 fluxes suggest that northern temperate coastal habitats with mixed vegetation, algal dominance, and their adjacent bare sediment areas are net sources of atmospheric CH_4 throughout the year.

As a result of extended periods of low temperature and temporal ice cover, the median annual fluxes were at the lower end compared to coastal wetland and tidal flat CH_4 emissions globally (Rosentreter et al., 2021b). However, in summer, CH_4 emissions of $\geq 100 \mu\text{mol CH}_4 \text{ m}^{-2} \text{ day}^{-1}$ across all habitats were comparable to, or even higher than, those reported from similar (Lundevall-Zara et al., 2021) or other vegetated coastal ecosystems (Al-Haj & Fulweiler, 2020; Rosentreter et al., 2021b). During these periods, large amounts of carbon are turned over in the habitats studied here (Attard et al., 2019a, 2019b), and macrophyte tissues become a direct component of local sediment organic matter pools (Marcelina et al., 2018) that favor local CH_4 production (Dale et al., 2019; Wallenius et al., 2021). Despite these seasonally relevant CH_4 emissions, there is still a paucity of data from northern temperate coastal habitats in general, and they are exceedingly underrepresented in current global CH_4 budgets. Yet, just in the Baltic Sea, the potential distribution

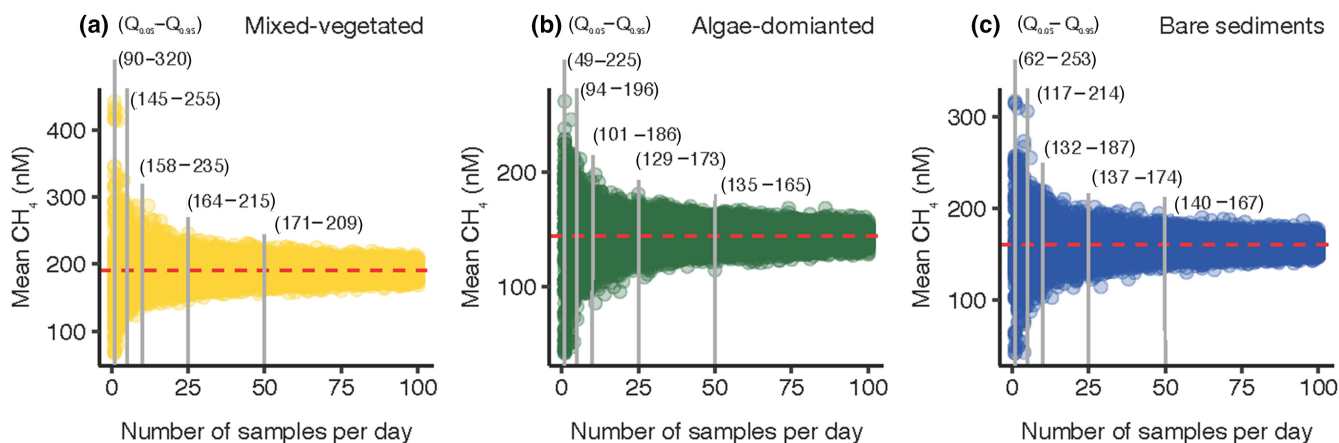


FIGURE 5 The mean surface water CH_4 concentration obtained by bootstrapping the population of measured CH_4 concentrations, with a sampling number ranging from 1 to 100 samples per day, and 200 replicates for each number of samples. The numbers in parentheses show the 5th–95th percentiles [$Q_{0.05}$ – $Q_{0.95}$] for 5, 10, 25, and 50 samples. The red dashed line shows the true daily mean of the measured CH_4 concentrations. Bootstrapping results are shown for of the mixed-vegetated (a), algae-dominated (b) and bare sediment (c) habitat in August. Bootstrapping results of all other months in Table S5

area in waters of <5 m depth is almost 30,000 km² (HELCOM, 2013; Jakobsson et al., 2019), and, thus, equals 22% of the global areal extent of mangroves (Bunting et al., 2018) or 19% that of sea-grass meadows (McKenzie et al., 2020). Thus, we: (a) postulate that nearshore habitats in northern temperate regions are understudied but seasonally relevant emitters of CH₄ to the atmosphere; (b) encourage including these habitats in future coastal CH₄ emission estimates, while also recognizing their pronounced seasonality; and (c) hypothesize that including these habitats amplifies the global ocean CH₄ budget significantly, especially when considering that macroalgae habitats alone contribute most (>50%) to the total global extent of coastal vegetation (Duarte et al., 2013).

4.8 | Uncertainties in coastal CH₄ distribution and future research directions

Variations of surface water CH₄ concentrations and resulting sea-air fluxes reflecting the heterogeneous nature of coastal environments currently complicate generalizing regional patterns and upscaling attempts globally. Given the CH₄ distribution patterns identified in this study, we encourage several aspects to be considered to refine large-scale coastal CH₄ emission budgets.

First, studies currently used for global coastal CH₄ budgets have a site-selective bias due to their particular relevance in providing a service (e.g., they are interesting from a blue carbon perspective) and for other practical reasons like the accessibility of the study area. Here, we provided evidence that northern temperate coastal habitats, which are presently understudied for their contribution to CH₄ fluxes (e.g., algal communities on rocky shores), can be seasonally relevant sources of atmospheric CH₄. Similar measurements should be extended to additional coastal environments and geolocations to confirm the global relevance of their CH₄ emissions. The spatial heterogeneity of coastal habitats provides an opportunity for measurements along environmental gradients, with great potential to increase inference across scales (Snelgrove et al., 2014).

Second, new technical approaches have to be embraced to better understand the high temporal variability of the CH₄ distribution and the underlying processes in coastal environments. The use of continuous rather than time-averaged measurements helps to account for short-term temporal variations by diel cycles or peak events (Call et al., 2015; Maher et al., 2013; Rosentreter et al., 2018), and reduces uncertainties when establishing diel budgets. The high-resolution measurements across multiple seasons and the identification of dependencies on environmental variables have also bearings for predicting future CH₄ emissions under various changing environmental conditions.

Third, net annual CH₄ fluxes are influenced by temporal variations throughout the year. Thus, to increase confidence when compiling data for global coastal CH₄ budgets, better seasonal coverage of coastal CH₄ needs to be combined with the recognition that reported mean values (both CH₄ concentrations and emissions) might be biased toward sampling in a particular period only. As the

seasonal behavior of CH₄ is highly site-specific, the variations need to be considered for each habitat type and geolocation.

Lastly, measurements of CH₄ emission from northern temperate and high-latitude coastal habitats should be acknowledged in future emission budgets. Climate change occurs particularly fast in northern hemisphere mid-latitude (Cohen et al., 2014) and high-latitude (Screen & Simmonds, 2010; Serreze et al., 2009) regions. Specifically, as Earth approaches an average warming of 2°C, some northern hemisphere high-latitude regions are expected to reach 4°C annual warming, outpacing the global average (Overland et al., 2014; Post et al., 2019). Although we could show a nonlinear behavior of CH₄ emissions with temperature, future studies aiming at resolving questions associated with climate change need to consider inter-annual rather than seasonal variations in CH₄ emissions and the balance of all important carbon pathways that influence CH₄ production pathways (Yvon-Durocher et al., 2014).

5 | CONCLUSION

We conducted seasonal sampling campaigns of dissolved CH₄ concentrations and δ¹³C-CH₄ values using a fast-response automated gas equilibrator and CRDS system across three globally pervasive vegetated and nonvegetated coastal habitats. As the first study to compare high-resolution measurements across neighboring habitats, we highlight unprecedented spatiotemporal variability of the CH₄ distribution driven by habitat-specific CH₄ production and consumption pathways, seasonal temperature dependencies, and short-term fluctuations. A bootstrapping analysis on the continuous data revealed that scaling the CH₄ distribution from few samples involves large errors, and at least ~50 samples per day are needed to achieve accurate emission estimates. Failing to include such high-resolution measurements in future global CH₄ assessments may result in a continued systematic bias of regional and global estimates due to the lack of measurements representative for the coastal ecosystem mosaic—a highly heterogeneous environment in space and time. Ultimately, a better understanding of the habitat-specific contribution to the global CH₄ emission budget would improve efforts to address climate change, such as by revealing the net potential of coastal blue carbon habitats to sequester carbon.

ACKNOWLEDGMENTS

This research is part of the Baltic Bridge strategic partnership between the Stockholm University and the University of Helsinki and the Centre for Coastal Ecosystem and Climate Research (CoastClim). We thank the staff at Stockholm Universities' field station Askö for their logistical support, and Joakim Hansen for the help with benthic macrophyte surveys. We appreciate constructive feedback from Robinson W. Fulweiler and Brett F. Thornton during manuscript preparation.

CONFLICT OF INTEREST

The authors declare that they have no competing interests.

AUTHOR CONTRIBUTIONS

F.R., C.H., and A.N. involved in conceptualization; F.R., X.S., M.C.G., and C.H. involved in methodology; C.H., A.N., J.P., and V.B. involved in material and logistics; F.R., X.S., J.P., S.B., E.B., F.N., and C.H. investigated the study; F.R., X.S., J.P., C.H., and A.N. contributed in data interpretation and data analysis; F.R., X.S., C.H., and A.N. wrote the original draft; all authors reviewed and edited the manuscript.

ORCID

Florian Roth  <https://orcid.org/0000-0003-4004-5863>

Xiaole Sun  <https://orcid.org/0000-0003-2391-5572>

John Prytherch  <https://orcid.org/0000-0003-1209-289X>

Volker Brüchert  <https://orcid.org/0000-0002-8956-3840>

Stefano Bonaglia  <https://orcid.org/0000-0003-4366-0677>

Elias Broman  <https://orcid.org/0000-0001-9005-5168>

Francisco Nascimento  <https://orcid.org/0000-0003-3722-1360>

Alf Norkko  <https://orcid.org/0000-0002-9741-4458>

Christoph Humborg  <https://orcid.org/0000-0002-0649-5599>

REFERENCES

- Al-Haj, A. N., & Fulweiler, R. W. (2020). A synthesis of methane emissions from shallow vegetated coastal ecosystems. *Global Change Biology*, 26, 2988–3005. <https://doi.org/10.1111/gcb.15046>
- Attard, K. M., Rodil, I. F., Berg, P., Norkko, J., Norkko, A., & Glud, R. N. (2019a). Seasonal metabolism and carbon export potential of a key coastal habitat: The perennial canopy-forming macroalga *Fucus vesiculosus*. *Limnology and Oceanography*, 64, 149–164. <https://doi.org/10.1002/lno.11026>
- Attard, K. M., Rodil, I. F., Glud, R. N., Berg, P., Norkko, J., & Norkko, A. (2019b). Seasonal ecosystem metabolism across shallow benthic habitats measured by aquatic eddy covariance. *Limnology and Oceanography Letters*, 4, 79–86. <https://doi.org/10.1002/lo2.10107>
- Banerjee, K., Paneerselvam, A., Ramachandran, P., Ganguly, D., Singh, G., & Ramesh, R. (2018). Seagrass and macrophyte mediated CO₂ and CH₄ dynamics in shallow coastal waters. *PLoS One*, 13, e0203922. <https://doi.org/10.1371/journal.pone.0203922>
- Barker, J. F., & Fritz, P. (1981). Carbon isotope fractionation during microbial methane oxidation. *Nature*, 293, 289–291. <https://doi.org/10.1038/293289a0>
- Barnes, R. O., & Goldberg, E. D. (1976). Methane production and consumption in anoxic marine sediments. *Geology*, 4, 297. [https://doi.org/10.1130/0091-7613\(1976\)4<297:MPACIA>2.0.CO;2](https://doi.org/10.1130/0091-7613(1976)4<297:MPACIA>2.0.CO;2)
- Bastviken, D., Ejlertsson, J., & Tranvik, L. (2002). Measurement of methane oxidation in lakes: A comparison of methods. *Environmental Science and Technology*, 36, 3354–3361. <https://doi.org/10.1021/es010311p>
- Bunting, P., Rosenqvist, A., Lucas, R., Rebelo, L.-M., Hilarides, L., Thomas, N., Hardy, A., Itoh, T., Shimada, M., & Finlayson, C. (2018). The global Mangrove watch—A new 2010 global baseline of Mangrove extent. *Remote Sensing*, 10, 1669. <https://doi.org/10.3390/rs10101669>
- Call, M., Maher, D. T., Santos, I. R., Ruiz-Halpern, S., Mangion, P., Sanders, C. J., Erler, D. V., Oakes, J. M., Rosentreter, J., Murray, R., & Eyre, B. D. (2015). Spatial and temporal variability of carbon dioxide and methane fluxes over semi-diurnal and spring-neap-spring timescales in a mangrove creek. *Geochimica Et Cosmochimica Acta*, 150, 211–225. <https://doi.org/10.1016/j.gca.2014.11.023>
- Call, M., Santos, I. R., Dittmar, T., de Rezende, C. E., Asp, N. E., & Maher, D. T. (2019). High pore-water derived CO₂ and CH₄ emissions from a macro-tidal mangrove creek in the Amazon region. *Geochimica et Cosmochimica Acta*, 247, 106–120. <https://doi.org/10.1016/j.gca.2018.12.029>
- Cardinale, B. J., Srivastava, D. S., Emmett Duffy, J., Wright, J. P., Downing, A. L., Sankaran, M., & Jouseau, C. (2006). Effects of biodiversity on the functioning of trophic groups and ecosystems. *Nature*, 443, 989–992. <https://doi.org/10.1038/nature05202>
- Cohen, J., Screen, J. A., Furtado, J. C., Barlow, M., Whittleston, D., Coumou, D., Francis, J., Dethloff, K., Entekhabi, D., Overland, J., & Jones, J. (2014). Recent arctic amplification and extreme mid-latitude weather. *Nature Geoscience*, 7, 627–637. <https://doi.org/10.1038/ngeo2234>
- Dale, A. W., Flury, S., Fossing, H., Regnier, P., Røy, H., Scholze, C., & Jørgensen, B. B. (2019). Kinetics of organic carbon mineralization and methane formation in marine sediments (Aarhus Bay, Denmark). *Geochimica Et Cosmochimica Acta*, 252, 159–178. <https://doi.org/10.1016/j.gca.2019.02.033>
- Denfeld, B. A., Baulch, H. M., del Giorgio, P. A., Hampton, S. E., & Karlsson, J. (2018). A synthesis of carbon dioxide and methane dynamics during the ice-covered period of northern lakes. *Limnology and Oceanography Letters*, 3, 117–131. <https://doi.org/10.1002/lo2.10079>
- Dias, G. M., Christofoletti, R. A., Kitazawa, K., & Jenkins, S. R. (2018). Environmental heterogeneity at small spatial scales affects population and community dynamics on intertidal rocky shores of a threatened bay system. *Ocean and Coastal Management*, 164, 52–59. <https://doi.org/10.1016/j.ocecoaman.2017.12.001>
- Duarte, C. M., Losada, I. J., Hendriks, I. E., Mazarrasa, I., & Marbà, N. (2013). The role of coastal plant communities for climate change mitigation and adaptation. *Nature Climate Change*, 3, 961–968. <https://doi.org/10.1038/nclimate1970>
- Duarte, C. M., Middelburg, J. J., & Caraco, N. (2005). Major role of marine vegetation on the oceanic carbon cycle. *Biogeosciences*, 2, 1–8. <https://doi.org/10.5194/bg-2-1-2005>
- Ducharme-Riel, V., Vachon, D., del Giorgio, P. A., & Prairie, Y. T. (2015). The relative contribution of winter under-ice and summer hypolimnetic CO₂ accumulation to the annual CO₂ emissions from Northern Lakes. *Ecosystems*, 18, 547–559. <https://doi.org/10.1007/s10021-015-9846-0>
- Dutta, M. K., Mukherjee, R., Jana, T. K., & Mukhopadhyay, S. K. (2015). Biogeochemical dynamics of exogenous methane in an estuary associated to a mangrove biosphere. *Marine Chemistry*, 170, 1–10. <https://doi.org/10.1016/j.marchem.2014.12.006>
- Gülzow, W., Rehder, G., Schneider v. Deimling, J., Seifert, T., & Tóth, Z. (2013). One year of continuous measurements constraining methane emissions from the Baltic Sea to the atmosphere using a ship of opportunity. *Biogeosciences*, 10, 81–99. <https://doi.org/10.5194/bg-10-81-2013>
- Hartmann, J. F., Gentz, T., Schiller, A., Greule, M., Grossart, H. P., Ionescu, D., Keppler, F., Martinez-Cruz, K., Sepulveda-Jauregui, A., & Isenbeck-Schröter, M. (2018). A fast and sensitive method for the continuous in situ determination of dissolved methane and its $\delta^{13}\text{C}$ -isotope ratio in surface waters. *Limnology and Oceanography: Methods*, 16, 273–285. <https://doi.org/10.1002/lom3.10244>
- Haugen, D. A. (1973). *Workshop on micrometeorology*. American Meteorological Society.
- HELCOM. (2013). Red List of Baltic Sea underwater biotopes, habitats, and biotope complexes.
- Hewitt, J. E., Thrush, S. F., & Dayton, P. D. (2008). Habitat variation, species diversity and ecological functioning in a marine system. *Journal of Experimental Marine Biology and Ecology*, 366, 116–122. <https://doi.org/10.1016/j.jembe.2008.07.016>
- Hofmann, H., Federwisch, L., & Peeters, F. (2010). Wave-induced release of methane: Littoral zones as source of methane in lakes. *Limnology and Oceanography*, 55, 1990–2000. <https://doi.org/10.4319/lo.2010.55.5.1990>

- Holland, K. T., & Elmore, P. A. (2008). A review of heterogeneous sediments in coastal environments. *Earth-Science Rev*, 89, 116–134. <https://doi.org/10.1016/j.earscirev.2008.03.003>
- Humborg, C., Geibel, M. C., Sun, X., McCrackin, M., Mörth, C.-M., Stranne, C., Jakobsson, M., Gustafsson, B., Sokolov, A., Norkko, A., & Norkko, J. (2019). High emissions of carbon dioxide and methane from the coastal Baltic Sea at the end of a summer heat wave. *Frontiers in Marine Science*, 6, 1–14. <https://doi.org/10.3389/fmars.2019.00493>
- Husson, F., Josse, J., Le, S., Mazet, J., & Husson, M. F. (2016). Package 'FactoMineR'. *An R Packag*, 96, 698.
- Jähne, B., Münnich, K. O., Böisinger, R., Dutzi, A., Huber, W., & Libner, P. (1987). On the parameters influencing air-water gas exchange. *Journal of Geophysical Research*, 92, 1937. <https://doi.org/10.1029/JC092iC02p01937>
- Jakobsson, M., Stranne, C., O'Regan, M., Greenwood, S. L., Gustafsson, B., Humborg, C., & Weidner, E. (2019). Bathymetric properties of the Baltic Sea. *Ocean Science*, 15, 905–924. <https://doi.org/10.5194/os-15-905-2019>
- Karlsson, J., Giesler, R., Persson, J., & Lundin, E. (2013). High emission of carbon dioxide and methane during ice thaw in high latitude lakes. *Geophysical Research Letters*, 40, 1123–1127. <https://doi.org/10.1002/grl.50152>
- Kassambara, A., & Mundt, F. (2017). Package 'factoextra'. *Extr. Vis. results Multivar. data Anal.* 76.
- Kim, J., Verma, S. B., & Billesbach, D. P. (2001). Seasonal variation in methane emission from a temperate Phragmites-dominated marsh: Effect of growth stage and plant-mediated transport. *Global Change Biology*, 5, 433–440. <https://doi.org/10.1046/j.1365-2486.1999.00237.x>
- Kim, J., Verma, S. B., Billesbach, D. P., & Clement, R. J. (1998). Diel variation in methane emission from a midlatitude prairie wetland: Significance of convective throughflow in Phragmites australis. *Journal of Geophysical Research Atmospheres*, 103, 28029–28039. <https://doi.org/10.1029/98JD02441>
- Koch, E. W. (2001). Beyond light: Physical, geological, and geochemical parameters as possible submersed aquatic vegetation habitat requirements. *Estuaries*, 24, 1. <https://doi.org/10.2307/1352808>
- Laurila, T. (2021). ICOS ATC CH4 Release, Utö - Baltic sea (57.0 m), 2018-03-09-2021-01-31. <https://hdl.handle.net/11676/m67T4icmvChEfpzz-WOCH4FB>
- Lenth, R., Singmann, H., Love, J., Buerkner, P., & Herve, M. (2019). Package 'emmeans'.
- Li, Y., Fichot, C. G., Geng, L., Scarratt, M. G., & Xie, H. (2020). The contribution of methane photoproduction to the oceanic methane paradox. *Geophysical Research Letters*, 47, 1–10. <https://doi.org/10.1029/2020GL088362>
- Lundevall-Zara, M., Lundevall-Zara, E., & Brüchert, V. (2021). Sea-air exchange of methane in shallow inshore areas of the Baltic Sea. *Frontiers in Marine Science*, 8, 1–20. <https://doi.org/10.3389/fmars.2021.657459>
- Ma, X., Sun, M., Lennartz, S. T., & Bange, H. W. (2020). A decade of methane measurements at the Boknis Eck time series station in Eckernförde Bay (southwestern Baltic Sea). *Biogeosciences*, 17, 3427–3438. <https://doi.org/10.5194/bg-17-3427-2020>
- Maher, D. T., Cowley, K., Santos, I. R., Macklin, P., & Eyre, B. D. (2015). Methane and carbon dioxide dynamics in a subtropical estuary over a diel cycle: Insights from automated in situ radioactive and stable isotope measurements. *Marine Chemistry*, 168, 69–79. <https://doi.org/10.1016/j.marchem.2014.10.017>
- Maher, D. T., Santos, I. R., Leuven, J. R. F. W., Oakes, J. M., Erlor, D. V., Carvalho, M. C., & Eyre, B. D. (2013). Novel use of cavity ring-down spectroscopy to investigate aquatic carbon cycling from microbial to ecosystem scales. *Environmental Science and Technology*, 47, 12938–12945. <https://doi.org/10.1021/es4027776>
- Marcelina, Z., Adam, S., & Pierre, R. (2018). Spatial and temporal variability of organic matter sources and food web structure across benthic habitats in a low diversity system (southern Baltic Sea). *Journal of Sea Research*, 141, 47–60. <https://doi.org/10.1016/j.seares.2018.05.007>
- McKenzie, L. J., Nordlund, L. M., Jones, B. L., Cullen-Unsworth, L. C., Roelfsema, C., & Unsworth, R. K. F. (2020). The global distribution of seagrass meadows. *Environmental Research Letters*, 15, 074041. <https://doi.org/10.1088/1748-9326/ab7d06>
- McLeod, E., Chmura, G. L., Bouillon, S., Salm, R., Björk, M., Duarte, C. M., Lovelock, C. E., Schlesinger, W. H., & Silliman, B. R. (2011). A blueprint for blue carbon: Toward an improved understanding of the role of vegetated coastal habitats in sequestering CO₂. *Frontiers in Ecology and the Environment*, 9, 552–560. <https://doi.org/10.1890/110004>
- Medvedev, I. P., Rabinovich, A. B., & Kulikov, E. A. (2016). Tides in three enclosed basins: The Baltic, Black, and Caspian Seas. *Frontiers in Marine Science*, 3, 46. <https://doi.org/10.3389/fmars.2016.00046>
- Murase, J., & Sugimoto, A. (2005). Inhibitory effect of light on methane oxidation in the pelagic water column of a mesotrophic lake (Lake Biwa, Japan). *Limnology and Oceanography*, 50, 1339–1343. <https://doi.org/10.4319/lo.2005.50.4.1339>
- Nirmal Rajkumar, A., Barnes, J., Ramesh, R., Purvaja, R., & Upstill-Goddard, R. C. (2008). Methane and nitrous oxide fluxes in the polluted Adyar River and estuary, SE India. *Marine Pollution Bulletin*, 56, 2043–2051. <https://doi.org/10.1016/j.marpolbul.2008.08.005>
- Omstedt, A., Pettersen, C., Rodhe, J., & Winsor, P. (2004). Baltic Sea climate: 200 yr of data on air temperature, sea level variation, ice cover, and atmospheric circulation. *Climate Research*, 25, 205–216. <https://doi.org/10.3354/cr025205>
- Ortega, A., Gerdali, N. R., Alam, I., Kamau, A. A., Acinas, S. G., Logares, R., Gasol, J. M., Massana, R., Krause-Jensen, D., & Duarte, C. M. (2019). Important contribution of macroalgae to oceanic carbon sequestration. *Nature Geoscience*, 12, 748–754. <https://doi.org/10.1038/s41561-019-0421-8>
- Overland, J. E., Wang, M., Walsh, J. E., & Stroeve, J. C. (2014). Future Arctic climate changes: Adaptation and mitigation time scales. *Earth's Future*, 2, 68–74. <https://doi.org/10.1002/2013EF000162>
- Phelps, A. R., Peterson, K. M., & Jeffries, M. O. (1998). Methane efflux from high-latitude lakes during spring ice melt. *Journal of Geophysical Research Atmospheres*, 103, 29029–29036. <https://doi.org/10.1029/98JD00044>
- Post, E., Alley, R. B., Christensen, T. R., Macias-Fauria, M., Forbes, B. C., Gooseff, M. N., Iler, A., Kerby, J. T., Laidre, K. L., Mann, M. E., Olofsson, J., Stroeve, J. C., Ulmer, F., Virginia, R. A., & Wang, M. (2019). The polar regions in a 2°C warmer world. *Science Advances*, 5, eaaw9883. <https://doi.org/10.1126/sciadv.aaw9883>
- Precht, E., & Huettel, M. (2004). Rapid wave-driven advective pore water exchange in a permeable coastal sediment. *Journal of Sea Research*, 51, 93–107. <https://doi.org/10.1016/j.seares.2003.07.003>
- R Core Team. (2021). *R: A language and environment for statistical computing*. R Foundation for Statistical Computing.
- Reeburgh, W. S. (1983). Rates of biogeochemical processes in anoxic sediments. *Annual Review of Earth and Planetary Sciences*, 11, 269–298. <https://doi.org/10.1146/annurev.ea.11.050183.001413>
- Rodil, I. F., Attard, K. M., Gustafsson, C., & Norkko, A. (2021). Variable contributions of seafloor communities to ecosystem metabolism across a gradient of habitat-forming species. *Marine Environment Research*, 167, 105321. <https://doi.org/10.1016/j.marenvres.2021.105321>
- Rosentreter, J. A., Al-Haj, A. N., Fulweiler, R. W., & Williamson, P. (2021a). Methane and nitrous oxide emissions complicate coastal blue carbon assessments. *Global Biogeochemical Cycles*, 35, 044034. <https://doi.org/10.1029/2020GB006858>
- Rosentreter, J. A., Borges, A. V., Deemer, B. R., Holgersson, M. A., Liu, S., Song, C., Melack, J., Raymond, P. A., Duarte, C. M., Allen, G. H., Olefeldt, D., Poulter, B., Battin, T. I., & Eyre, B. D. (2021b). Half of global methane emissions come from highly variable aquatic ecosystem sources. *Nature Geoscience*, 14(4), 225–230. <https://doi.org/10.1038/s41561-021-00715-2>

- Rosentreter, J. A., Maher, D. T., Erler, D. V., Murray, R. H., & Eyre, B. D. (2018). Methane emissions partially offset "blue carbon" burial in mangroves. *Science Advances*, 4, eaao4985. <https://doi.org/10.1126/sciadv.aao4985>
- Rudd, J. W. M., Furrutani, A., Flett, R. J., & Hamilton, R. D. (1976). Factors controlling methane oxidation in shield lakes: The role of nitrogen fixation and oxygen concentration. *Limnology and Oceanography*, 21, 357–364. <https://doi.org/10.4319/lo.1976.21.3.0357>
- Schmale, O., Schneider Von Deimling, J., Gülzow, W., Nausch, G., Waniek, J. J., & Rehder, G. (2010). Distribution of methane in the water column of the Baltic Sea. *Geophysical Research Letters*, 37, 1–5. <https://doi.org/10.1029/2010GL043115>
- Screen, J. A., & Simmonds, I. (2010). The central role of diminishing sea ice in recent Arctic temperature amplification. *Nature*, 464, 1334–1337. <https://doi.org/10.1038/nature09051>
- Serreze, M. C., Barrett, A. P., Stroeve, J. C., Kindig, D. N., & Holland, M. M. (2009). The emergence of surface-based Arctic amplification. *The Cryosphere*, 3, 11–19. <https://doi.org/10.5194/tc-3-11-2009>
- Sheaves, M. (2009). Consequences of ecological connectivity: The coastal ecosystem mosaic. *Marine Ecology Progress Series*, 391, 107–115. <https://doi.org/10.3354/meps08121>
- Shindell, D. T., Faluvegi, G., Koch, D. M., Schmidt, G. A., Unger, N., & Bauer, S. E. (2009). Improved attribution of climate forcing to emissions. *Science*, 326, 716–718. <https://doi.org/10.1126/science.1174760>
- Sibly, R., Brown, J., & Kodric-Brown, A. (2012). *Metabolic ecology: A scaling approach*. Wiley-Blackwell.
- Sieczko, A. K., Duc, N. T., Schenk, J., Pajala, G., Rudberg, D., Sawakuchi, H. O., & Bastviken, D. (2020). Diel variability of methane emissions from lakes. *Proceedings of the National Academy of Sciences*, 117, 21488–21494. <https://doi.org/10.1073/pnas.2006024117>
- Snelgrove, P. V. R., Soetaert, K., Solan, M., Thrush, S., Wei, C.-L., Danovaro, R., Fulweiler, R. W., Kitazato, H., Ingole, B., Norkko, A., Parkes, R. J., & Volkenborn, N. (2018). Global carbon cycling on a heterogeneous seafloor. *Trends in Ecology & Evolution*, 33, 96–105. <https://doi.org/10.1016/j.tree.2017.11.004>
- Snelgrove, P. V. R., Thrush, S. F., Wall, D. H., & Norkko, A. (2014). Real world biodiversity–ecosystem functioning: A seafloor perspective. *Trends in Ecology & Evolution*, 29, 398–405. <https://doi.org/10.1016/j.tree.2014.05.002>
- Stein, A., Gerstner, K., & Kreft, H. (2014). Environmental heterogeneity as a universal driver of species richness across taxa, biomes and spatial scales. *Ecology Letters*, 17, 866–880. <https://doi.org/10.1111/ele.12277>
- Sveriges meteorologiska och hydrologiska institute. (2022). Oceanografiska observationer, Stationsnummer 2507 [WWW Document]. <https://www.smhi.se/data/oceanografi/ladda-ner-oceanografiska-observationer#param=seatemperature,stations=all,stationid=2507>
- Treude, T., Krüger, M., Boetius, A., & Jørgensen, B. B. (2005). Environmental control on anaerobic oxidation of methane in the gassy sediments of Eckernförde Bay (German Baltic). *Limnology and Oceanography*, 50, 1771–1786. <https://doi.org/10.4319/lo.2005.50.6.1771>
- van den Berg, M., van den Elzen, E., Ingwersen, J., Kosten, S., Lamers, L. P. M., & Streck, T. (2020). Contribution of plant-induced pressurized flow to CH₄ emission from a Phragmites fen. *Scientific Reports*, 10, 1–10. <https://doi.org/10.1038/s41598-020-69034-7>
- Wallenius, A. J., Dalcin Martins, P., Slomp, C. P., & Jetten, M. S. M. (2021). Anthropogenic and environmental constraints on the microbial methane cycle in coastal sediments. *Frontiers in Microbiology*, 12, 631621. <https://doi.org/10.3389/fmicb.2021.631621>
- Wanninkhof, R. (2014). Relationship between wind speed and gas exchange over the ocean revisited. *Limnology and Oceanography: Methods*, 12, 351–362. <https://doi.org/10.4319/lom.2014.12.351>
- Weber, T., Wiseman, N. A., & Kock, A. (2019). Global ocean methane emissions dominated by shallow coastal waters. *Nature Communications*, 10, 1–10. <https://doi.org/10.1038/s41467-019-12541-7>
- Wiesenburg, D. A., & Guinasso, N. L. (1979). Equilibrium solubilities of methane, carbon monoxide, and hydrogen in water and sea water. *Journal of Chemical and Engineering Data*, 24, 356–360. <https://doi.org/10.1021/je60083a006>
- Wilson, S. T., Bange, H. W., Arévalo-Martínez, D. L., Barnes, J., Borges, A. V., Brown, I., Bullister, J. L., Burgos, M., Capelle, D. W., Casso, M., De La Paz, M., Fariás, L., Fenwick, L., Ferrón, S., García, G., Glockzin, M., Karl, D. M., Kock, A., Laperriere, S., ... Rehder, G. (2018). An intercomparison of oceanic methane and nitrous oxide measurements. *Biogeosciences*, 15, 5891–5907. <https://doi.org/10.5194/bg-15-5891-2018>
- Yang, Z., Zhu, Y., Liu, T., Sun, Z., Ling, X., & Yang, J. (2019). Pumping effect of wave-induced pore pressure on the development of fluid mud layer. *Ocean Engineering*, 189, 106391. <https://doi.org/10.1016/j.oceaneng.2019.106391>
- Yvon-Durocher, G., Allen, A. P., Bastviken, D., Conrad, R., Gudas, C., St-Pierre, A., Thanh-Duc, N., & Del Giorgio, P. A. (2014). Methane fluxes show consistent temperature dependence across microbial to ecosystem scales. *Nature*, 507, 488–491. <https://doi.org/10.1038/nature13164>
- Zehnder, A. J. B., & Brock, T. D. (1980). Anaerobic methane oxidation: Occurrence and ecology. *Applied and Environment Microbiology*, 39, 194–204. <https://doi.org/10.1128/AEM.39.1.194-204.1980>
- Zhang, Y., & Xie, H. (2015). Photomineralization and photomethanification of dissolved organic matter in Saguenay River surface water. *Biogeosciences*, 12, 6823–6836. <https://doi.org/10.5194/bg-12-6823-2015>

SUPPORTING INFORMATION

Additional supporting information may be found in the online version of the article at the publisher's website.

How to cite this article: Roth, F., Sun, X., Geibel, M. C., Prytherch, J., Brüchert, V., Bonaglia, S., Broman, E., Nascimento, F., Norkko, A., & Humborg, C. (2022). High spatiotemporal variability of methane concentrations challenges estimates of emissions across vegetated coastal ecosystems. *Global Change Biology*, 28, 4308–4322. <https://doi.org/10.1111/gcb.16177>